ANOMALOUS LOW STATES AND LONG TERM VARIABILITY IN THE BLACK HOLE BINARY LMC X-3

Alan P. Smale and Patricia T. Boyd
Astrophysics Science Division, NASA Goddard Space Flight Center, Greenbelt, MD 20771
Received 2012 January 11; accepted 2012 July 12

ABSTRACT

Rossi X-ray Timing Explorer observations of the black hole binary LMC X-3 reveal an extended very low X-ray state lasting from 2003 December 13 until 2004 March 18, unprecedented both in terms of its low luminosity (>15 times fainter than ever before seen in this source) and long duration (~3 times longer than a typical low/hard state excursion). During this event little to no source variability is observed on timescales of ~hours-weeks, and the X-ray spectrum implies an upper limit of 1.2×10^{35} erg s^{-1}. Five years later another extended low state occurs, lasting from 2008 December 11 until 2009 June 17. This event lasts nearly twice as long as the first, and while significant variability is observed, the source remains reliably in the low/hard spectral state for the ~188 day duration. These episodes share some characteristics with the "anomalous low states" in the neutron star binary Her X-1. The average period and amplitude of the variability of LMC X-3 have different values between these episodes. We characterize the long-term variability of LMC X-3 before and after the two events using conventional and nonlinear time series analysis methods, and show that, as is the case in Her X-1, the characteristic amplitude of the variability is related to its characteristic timescale. Furthermore, the relation is in the same direction in both systems. This suggests that a similar mechanism gives rise to the long-term variability, which in the case of Her X-1 is reliably modeled with a tilted, warped precessing accretion disk.

Subject headings: accretion, accretion disks - binaries: close - black hole physics - stars: individual (LMC X-3) - X-rays: binaries

1. INTRODUCTION

LMC X-3 is a bright (up to 3×10^{38} erg s^{-1}) black hole candidate (BHC) in the Large Magellanic Cloud that is unique among persistent BHCs in its high variability on timescales from days to years. The mechanism governing this variability, and even the method by which the compact object accretes mass from its companion, remains highly uncertain after decades of observations and analysis. It is typically observed in the high/soft state, with an X-ray spectrum qualitatively similar to that of other BHCs in the soft state: an "ultrasoft" component and a hard X-ray tail (e.g. Chen & Taam (1996)). Occasional, brief low/hard states show canonical spectral and timing behavior, with a simple power law spectrum with photon index $\Gamma=1.69\pm0.02$, a source luminosity at 50 kpc of $(5-16) \times 10^{36}$ erg s^{-1} (2-10 keV), and strong broadband (0.01-100 Hz) time variability, with fractional rms amplitude of $40\pm4\%$ and a quasi-periodic oscillation peak at 0.46 ± 0.02 Hz with rms amplitude ~14% (Boyd et al. 2000).

The optical counterpart shows a large velocity range with semi-amplitude K=235 km s^{-1} through its 1.7-day orbit. The lack of eclipses implies an orbital inclination < 70°, and a compact object mass of ~7M$_\odot$ (Cowley et al. 1983). Historical UV and optical spectra were used to constrain the additional variable flux, presumably from the accretion disk, suggesting that at some orientations the disk is responsible for nearly half of the UV/optical flux from the system (Cowley et al. 1994). IUE and FOS spectra from 1992 show LMC X-3 to have a UV line spectrum containing only weak emission features, unusual for the presumed B3V mass donor star. The data show that as LMC X-3 becomes brighter in the UV it also becomes bluer. Similarly, the emis-

sion line strengths increase with UV flux. Cowley et al. (1991) argue that this behavior is consistent with the accretion disk being seen at varying observing angles, at some times obscuring and at other times revealing the hot central part as it precesses. However, analysis of UV continuum and line spectra from *IUE* and *HST*/FOS (Cowley et al. 1994) timed to sample the long term variability cycle showed that the UV and optical luminosity never reached the expected maximum. The authors speculate than LMC X-3 may have undergone an anomalous low state, however insufficient data were available to test this hypothesis.

The X-ray contribution to the UV/optical spectrum complicates a determination of the companion star's spectral type. Soria et al. (2001) analyzed *XMM-Newton* Optical Monitor observations taken on 2000 April 19, when the source was near a low/hard state (Boyd & Smale 2004). Fitting their results to evolutionary models for the companion, Soria et al derived a spectral type of B5IV. High resolution optical spectroscopy of the companion star, with the appropriate corrections for X-ray heating, leads to a similar spectral type estimate of B5V (Val-Baker, Norton & Negueruela 2007). The mass accretion mechanism is therefore most likely Roche lobe overflow, with minimal contribution from its stellar wind. In a related analysis, Wu et al. (2001) analyzed *XMM-Newton* RGS and EPIC data from 2000 February–June, during the transition into and out of a low/hard state. Spectral fits to the RGS data indicate that the line of sight column density N_H is $< 10^{21}$ cm^{-2}, inconsistent with the expectation of a larger value if the companion had a strong stellar wind. In addition, no obvious emission lines were observed, consistent with no previous epochs of wind matter ejection. Soria et al. (2001) conclude that LMC X-3 accretes via Roche lobe overflow from the companion, as opposed to via a strong stellar

Electronic address: alan.smale@nasa.gov, padi.boyd@nasa.gov

wind.

LMC X-3 belongs to a class of binaries that show high amplitude X-ray variability on time scales much longer than their orbital periods. Reports of a ~198 (or perhaps ~99) day superorbital periodicity in early data (Cowley et al. 1991) were based on unevenly spaced data sets with gaps. More recent continuous monitoring initiated with *RXTE*'s All-Sky Monitor (ASM) in 1995 has led to the realization that the source shows a much more complex and less strictly periodic long-term variability (Paul, Kitamoto & Makino 2000; Wilms et al. 2001; Boyd & Smale 2004).

Wilms et al. (2001) analyzed *RXTE* ASM light curves along with Proportional Counter Array (PCA) spectra and found that LMC X-3 exhibits recurrent transitions from the soft to the hard state. They argued in favor of a wind-driven limit cycle driving the observed variability, and against a large accretion disk self-shadowing due to a warp.

From the analysis of 6 years of optical V and B data, partially overlapping with *RXTE* ASM monitoring, Brocksopp, Groot & Wilms (2001) found that the long-term optical and X-ray variability are correlated, with the X-ray lagging the optical by about 5 to 10 days. They argue that this supports the mechanism of variable mass accretion rate giving rise to the long-term variability and suggest an accretion disk wind instability limit cycle to generate the observed behavior.

Several other X-ray binaries show large amplitude variations in their X-ray fluxes on timescales significantly longer than their orbital periods. The canonical example is the eclipsing X-ray pulsar Her X-1, in which the long-term X-ray light curve is dominated by a high amplitude, double-peaked 35-day variation. The main features of this periodicity can be successfully explained by the presence of a warped or inclined accretion disk precessing with respect to the binary orbital plane (Priedhorsky & Holt 1987). Other systems that show nearly periodic variations at least an order of magnitude longer than the orbital period include the accreting X-ray pulsars SMC X-1 (50-60 dy; Gruber & Rothschild (1984); Wojdowski, Clark & Kallman (2000), but see Clarkson et al. (2003)) and LMC X-4 (30.5 dy; Lang et al. (1981), but see Trowbridge, Nowak & Wilms (2007)), as well as the paradigmatic disk jet source SS 433 (Fabian & Rees 1979; Abell & Margon 1979). In almost all cases, the observed behavior is found to be more complex than the prediction of strict periodicity from a simple precessing disk model. Even the canonical source, Her X-1, has been observed to undergo prolonged anomalous low states (ALS's) in which the long-term X-ray variation is only marginally detected, if at all (Still & Boyd 2004). More detailed modeling of the radiation-driven warping instability uncovered regions of physical parameter space that could give rise to unstable, apparently chaotic disk precession with no stable long-term period (Wijers & Pringle 1999; Ogilvie & Dubus 2001). Foulkes, Haswell & Murray (2010) performed a sophisticated numerical investigation using smoothed particle hydrodynamics (SPH) and found that warping occurs across a broader range of parameters and remains more stable than previously thought.

The organization of this paper is as follows. In Section 2, we describe the data set we used to study the long-term variability of LMC X-3 as well as our time series analysis methods, and results. We argue that the data support the interpretation that LMC X-3 underwent two ALS's and that the long-term behavior, as characterized by average excursion lengths and amplitudes, is measurably different between ALS's, in essentially the same manner as we previously observed in Her X-1. Section 3 discusses the implications of the similarities of long-term variability in terms of a period-amplitude relation that holds in both LMC X-3 and Her X-1. We also compare the period-amplitude relation of both systems with various nonlinear oscillator models. In Section 4 we present our conclusions on the existence of a period-amplitude relation in the long-term light curves of these two quite different X-ray binaries, and some potential further directions of investigation.

2. DATA ANALYSIS AND RESULTS

2.1. *The Overall Light Curve*

In this paper we make use of extensive archival data from the All-Sky Monitor (ASM) (Levine et al. 1996) and Proportional Counter Array (PCA) (Jahoda et al. 1996), on board the *Rossi X-ray Timing Explorer* satellite (*RXTE*) (Bradt, Rothschild & Swank 1993). The ASM is a set of three scanning shadow cameras which cover the 1.5–12.0 keV energy range in three broad bands. It scans most of the sky each 90-minute satellite orbit, collecting X-ray intensity measurements in 90 second dwells. Since the launch of *RXTE* in 1995 December the ASM has generated an impressive archive of high-quality, evenly sampled time series data on virtually all moderately bright X-ray sources. The ASM light curves can be used to explore variability timescales from days to decades. The PCA consists of five Xe Proportional Counting Units (PCUs) with a combined collecting area of about 6500 cm^2, and provides high time resolution and moderate spectral resolution in the 2-60 keV energy range.

The *RXTE* ASM light curve for LMC X-3 is remarkable in its completeness, and is a virtually uninterrupted, evenly sampled time series capturing the dramatic aperiodic variability from this unique source (Figure 1a). Typically, its X-ray flux is seen to vary smoothly and continuously through a fairly fixed range, from fractions of a count per second to just over 4 counts s^{-1} (for comparison, the Crab is approximately 74 counts s^{-1}). The timescale from one maximum to the next varies from as short as two months to longer than one year. In addition to this behavior, we note two unusual episodes of remarkably low count rate, each lasting for several months (Figure 1a).

For our analysis of long-term variability, we started from the ASM light curves available via the HEASARC. These contain data from each 90-second dwell, and include the calibration and filtering criteria applied by the ASM instrument team[1]. We rebinned to a sample time of 4 days, a bin size chosen to improve the signal to noise ratio and minimize the number of data gaps while preserving adequate sampling for the timescales of interest. Having used the most recent ASM data calibration available[2], we restricted our analysis to data taken up to and

---

[1] http://heasarc.gsfc.nasa.gov/docs/xte/ASM/asm_events.html
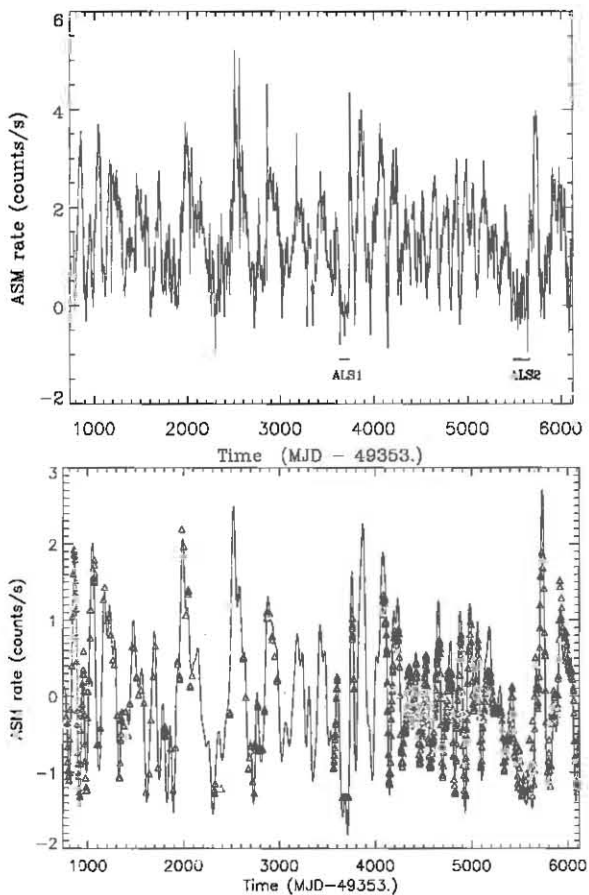[2] http://heasarc.gsfc.nasa.gov/docs/xte/asm_2010.html

FIG. 1.— (a) The ASM light curve of LMC X-3 from 1996 through 2010, summed into 4-dy bins. (b) The ASM light curve, smoothed as described in the text (solid line), shown together with all available PCA Standard2 data (triangles; one point per observation). Both data sets have been mean-subtracted, and the PCA data has been scaled to have the same maximum and minimum value as the ASM data. From this figure we conclude that smoothed ASM light curve provides a faithful representation of the overall source behavior, without adding spurious artifacts.

just beyond the 2010 recalibration to minimize variability due to unmodeled calibration drift. Our dataset thus covers the 14.75 years from 1996 January 5 through 2010 October 8.

For our analysis purposes, additional interpolation and filtering of the ASM light curve was required. Since we require a truly evenly spaced time series, the occasional sporadic gaps in the data were filled with random data with the same mean and standard deviation as the global dataset (only 18 data points out of 1,347 required this treatment, representing 1.3% of the total). A simple power spectrum of the dataset reveals that the majority of the power is at frequencies corresponding to periods of 50 days or more. The data were thus smoothed using a Fourier low-pass filter, attenuating this high-frequency noise. The resulting smoothed ASM light curve forms the basis of Figure 1b, and is the principal light curve we utilize for the bulk of the timing analysis described below.

The HEASARC public archive contains a wealth of observations of LMC X-3 performed using the *RXTE* PCA. From launch to the end of 2010 there were a total of 1161

observations of LMC X-3, yielding a total exposure time of 2.9 Msec. Since these were initiated in response to 19 successful Guest Observer pointed, monitoring, and Target of Opportunity proposals, they comprise a heterogeneous and unevenly spaced record. However, since early 2005 the time coverage of LMC X-3 has been outstanding, due to a succession of dedicated long-running monitoring campaigns. The number of PCUs operating at any given time is variable, and for the later datasets typically only two PCUs are collecting data during monitoring observations. During every *RXTE* observation two standard PCA data modes are used, in addition to user-specified modes chosen depending on the nature of the science investigation. Standard2 mode collects all 129 spectral channels with 16 second time resolution, and due to its presence in all datasets provides the core data we analyze here.

First, we use the complete PCA Standard2 data record to test the possibility that our ASM light curve smoothing technique introduces spurious variability, or fails to reproduce real long-term variability in the source. In Figure 1b we show the smoothed ASM light curve for LMC X-3, with the PCA data from all available *RXTE* pointed observations superimposed. For each PCA observation we plot a single point, which is the average, background-subtracted, Standard2 count rate per PCU during the entire good observing time for that observation. It is clear from Figure 1b that the gross morphology of the long term variability, i.e., the occurrence times and flux values of the extrema, as well as the overall character of the signal in between, are very well preserved by the smoothed ASM light curve.

Inspection of Figure 1 shows that LMC X-3 has undergone a complex and aperiodic evolution during almost fifteen years of continuous monitoring by *RXTE*. Much of the time the flux is changing slowly, smoothly and continuously between extremes. The mean-subtracted time series appears stationary; there is no evidence for the trends or modulations on ~10-yr timescales which have become apparent in other sources (Durant et al. 2010).

2.2. Extended Low States

Close examination of the ASM light curve reveals two long episodes of low count rate. The unusual nature of these episodes can be emphasized by plotting the logarithm of the ASM count rate versus time (Figure 2). For the purposes of this Figure we have added 2 to the mean-subtracted ASM rate so that the signal is always positive definite. The horizontal line indicates the level at which the flux is at least 1 standard deviation (1σ) below the mean value. When the data are plotted on this scale two things become clear: (1) the flux value when the signal experiences a minimum does not always go below even 1σ of the mean value, and varies considerably, and (2) there are two episodes where the source flux stays very low for times much longer than the typical minimum. We demarcate these episodes in Figure 2 using dashed vertical lines: the extended low-state intervals correspond to *RXTE* mission days 3633-3729 and 5458-5646 (which in turn correspond to MJDs 52986-53082 and 54811-54999, and calendar dates 2003 December 13-2004 March 18, and 2008 December 11-2009 June 17).

First, we compare these lows to the ensemble of lows in the system, to see if they can indeed be considered
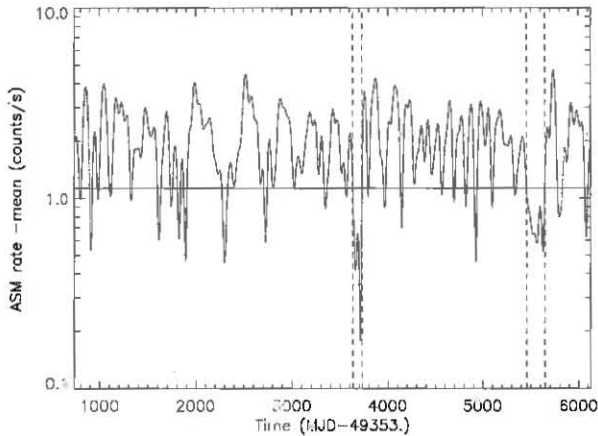
FIG. 2.— ASM light curve for the same time period as Figure 1, but with 2.0 added to the mean-subtracted count rate (see text), and the flux now displayed on a logarithmic scale. The behavior of the source when the flux is at least one standard deviation below the mean (horizontal line) varies appreciably from one minimum to the next. The two anomalously long episodes (dashed vertical lines) are readily apparent in this representation.

FIG. 3.— ASM and PCA light curves through the first anomalous low state. The ASM data are in 4-dy bins, unsmoothed; the PCA data are plotted as a single point per observation, with the measured count rate in the 3.0-25.0 keV band. Background subtraction for the PCA data does not include a contribution for the LMC diffuse background (see text).

anomalously long and low. To identify the durations of episodes where the signal is truly low, we locate times where the signal is 1σ below the mean. For each episode when the signal stays below this level, we use the local slope of the signal to linearly interpolate to estimate the times when the signal actually crosses this value, first in the downward and then in the upward direction. We use these crossing times to characterize the lengths of the lows. We find that there are 26 such low episodes, including the two unusually long episodes identified above. The shortest is 15 dy long. The longest lasts 188 dy. The average duration of all 26 low episodes is 37.4 ± 6.9 dy (where the error is defined as $\sigma/\sqrt{(n)}$). Excluding the two very long excursions and taking the average of the remaining 24 episodes gives a mean duration of 28.7 ± 2.3 dy. Using the same method of calculating crossing times, the duration of the first long low state is found to be 96 dy (3.4 times longer than the average and 6σ outlier), while the second lasts 188 dy (6.6 times longer than the average and 14σ outlier). Of the remaining excursions, 21 are <35 days in duration. There are three low excursion which last >35 days. They have lengths of 39 days (centered at RXTE mission day 1618 = MJD 50971), 52 days (centered at RXTE mission day 5802 = MJD 55155), and 62 days (centered at RXTE mission day 2304 = MJD 51657). PCA monitoring data covering the first two of these low excursions show a continuous, smooth change from higher fluxes to the low point and back up to higher flux levels, as seen in other typical low/hard excursions. There is insufficient PCA monitoring data through the third excursion, however the raw 4-day ASM rate changes smoothly into and out of this low, strongly suggesting that it too is typical.

We conclude that the two extended episodes of low flux we have identified are indeed anomalously long. For reasons we discuss in detail below, we refer to them as Anomalous Low States 1 and 2 for the remainder of this Paper.
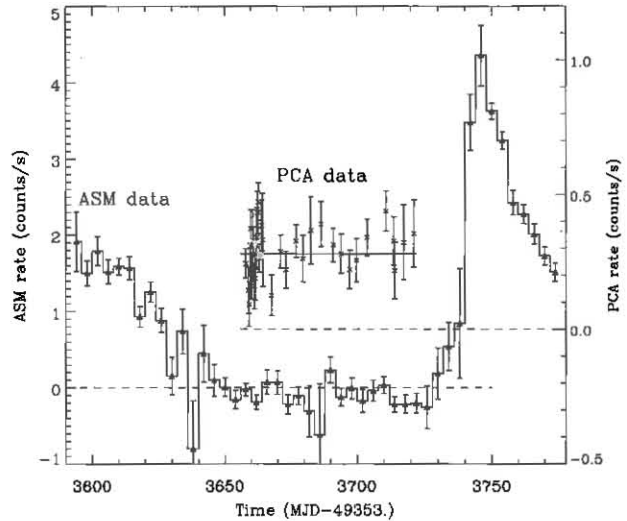
2.3. Spectral and Timing Analysis of Low States in LMC X-3

2.3.1. Anomalous Low State 1 (ALS1)

Fortuitously, we have excellent PCA coverage during ALS1. These observations were originally scheduled under *RXTE* observation ID (obsID) 80118-02 to be contemporaneous with an *INTEGRAL* study of the LMC (Gotz et al. 2006) supplemented with monitoring observations performed under the second part of obsID 80103-01 to search for hysteresis in state transitions, a study eventually completed using different data obtained in 2005 March (Smith, Dawson & Swank 2007). To the best of our knowledge, the PCA data we present in this paper have not been analyzed or published previously.

As shown in Figure 3, PCA data using various combinations of PCUs were obtained roughly every 3 days, for a total of 28 observations spread over 67 separate obsIDs, yielding 152 ksec of good data which span ∼64 days of the 96-day ALS (from 2004 January 7 through 2004 March 10). These PCA data were all obtained using Standard2 and Good Xenon data modes. To optimize the signal-to-noise ratio and enable the most consistent measurements of spectral parameters and flux, we limited our analysis to the 126.5 ksec of Standard2 data taken using PCUs 2 and 3, Layer 1. (The remaining good time includes data taken with a different combination of PCUs.)

The PCA data do not allow us to constrain the equivalent hydrogen column density N_H, and we thus fix it at 3.8×10^{20} cm^{-2} based on the accurate values obtained from radio measurements and from the O I edge (Nowak et al. 2001; Page et al. 2003; Smith, Dawson & Swank 2007). Over the energy range 3.0-25.0 keV, a good fit can then be obtained to the summed background-subtracted PCA spectrum of ALS1 using a simple power law model with photon index $\Gamma=1.7\pm0.2$, yielding a reduced chi-squared slightly under 1. Neither the fit statistic nor the residuals show a need to incorporate a second continuum component or a line

feature in the fit. For a distance of 50 kpc, the derived source luminosity during ALS1 is $L_{x(2-10keV)} = 4.2 \times 10^{35}$ erg s^{-1}, substantially lower than the typical luminosities derived for the "canonical" short low/hard states of LMC X-3 of $(1.9\text{-}15.7) \times 10^{36}$ erg s^{-1} (Boyd et al. 2000).

However, this standard background subtraction does not take into account the known large-scale diffuse emission from the LMC (see e.g. Points et al. (2001)). Although this emission is difficult to model and subtract out of our *RXTE* data, we can get a good indication of its contribution by examining the *RXTE* PCA slews to and from LMC X-3 for the ALS1 observations. We took two approaches to this, firstly by fitting all the ALS1 on-source data using the nearby slew data as "background", and secondly by carefully fitting spectra from chosen slews. For the latter, we selected a series of slews for which the Earth elevation angle was greater than 10° throughout, well away from PCU breakdown events, and using only data from PCU2 for which there are good slew data both onto and away from the source. Both approaches give similar results: somewhere between 70% and 100% of the measured flux from "LMC X-3" during ALS1 in fact originates in the nearby diffuse LMC emission. Conservatively, this would imply a maximum luminosity during ALS1 of ~1.2×10^{35} erg s^{-1}, ~15 times fainter than the minimum luminosity ever previously observed in a low/hard state, representing 1.3×10^{-4} L_{Edd}, However, within the errors, the data are consistent with the source having turned off completely.

2.3.2. *Anomalous Low State 2 (ALS2)*

Our PCA coverage of ALS2 is also excellent, due to monitoring of LMC X-3 carried out as part of the *RXTE* Core Observing Program. Under obsIDs 93113-01 and 94113-01 data were obtained every 3–4 days throughout the duration of ALS2 with good exposure times typically 2 ksec. Each of the individual spectra can be fit with a simple power law model with index ~1.7. Even the faintest of these spectra yields a source detection at levels comfortably higher than that of the diffuse LMC emission, and in fact significant variability continues to be observed in LMC X-3 within ALS2. Constructing an aggregate spectrum from the part of ALS2 where the flux levels are reliably the lowest and least variable (for the 87 days lasting from 2009 January 29 through 2009 April 26, incorporating 47 ksec of good data) and then fitting this spectrum with the equivalent hydrogen column density fixed at 3.8×10^{20} cm^{-2} as above, we achieve a good fit from 3.0-25.0 keV with a power law index of Γ=1.71±0.02. The fit has a reduced chi-squared of ~1, and a derived 2-10 keV flux of 4.62×10^{-11} erg cm^{-2} s^{-1}, corresponding to a luminosity of 1.38×10^{36} erg s^{-1} ($0.0015 L_{Edd}$) at the distance of LMC X-3. This luminosity level is lower than, but close to, those measured for the "canonical" low/hard states of LMC X-3 studied by Boyd et al. (2000).

In short, ALS2 is anomalous in duration, but not in the flux levels reached, which are similar to those seen in the more customary, shorter-duration low/hard states.

2.4. *Timing Analysis using Zero-Crossing Techniques*

In Figure 2, we provide dashed lines indicating where the anomalous low states begin and end. Visual inspection of the data before and after these ALS's suggests that the characteristic timescale and amplitude of the long-term variability may be different. It appears that the characteristic period is longer, and the amplitude higher before the source enters ALS1 than after it exits. The system then appears to favor a shorter-timescale, lower-amplitude variability until it enters ALS2. While there are insufficient cycles of variability to claim a new characteristic timescale after exiting ALS2, the ~two available cycles suggest a new longer timescale and higher amplitude than that present between the two ALS's.

In an attempt to quantify and characterize this change in the long-term variability, we consider the data outside of the ALS's as three distinct groupings. We label the data before entering ALS1 on *RXTE* day 3633 as "early". Data between the two ALS's (from *RXTE* days 3729-5458) are labeled "middle". The data after exiting ALS2 on day 5646 we label "late". For the purposes of characterizing the long-term variability characteristics we do not consider the data within the ALS's themselves.

Determining a timescale of interest from a nonperiodic signal requires different analysis tools from a traditional analysis. Fourier analysis is ideally suited to signals containing periodic, nearly sinusoidal variability, but for astrophysical signals the variability often does not fit this condition. Even a periodic signal as relatively simple as that from the Crab pulsar results in a complex Fourier transform that contains many harmonics as well as peaks at the fundamental frequency. This is due to the shape of its pulse profile, which is markedly steeper than a sine wave and has an interpulse offset from phase 0.5 (Rots, Jahoda & Lyne 2004). For signals in which the period and/or amplitude change with time, the use of a single Fourier transform becomes even more problematic and can lead to misidentifications of periodicities (Wilms et al. 2001; Paul, Kitamoto & Makino 2000).

In cases where strict periodicity is not present in a variable source, a short-time windowed Fourier transform (STWFT) has been used to analyze signals where the variability is presumed to be changing slowly with time. Even this assumption can potentially result in misleading conclusions about the fine details of the time evolution. In their reanalysis of the long-term evolution of SMC X-1, Trowbridge, Nowak & Wilms (2007) used a minimum-fitting procedure to determine the length of each individual superorbital cycle, They found that the long-term "period" could change by as much as a factor of two between adjacent cycles. Further, they found that the smoothing imposed by the STWFT algorithm masked the measurable cycle-to-cycle variability in the superorbital "period" for this source, which had led some authors (e.g. Clarkson et al. (2003)) to infer a slowly and smoothly varying long-term cycle perhaps due to the interaction of multiple disk warps in the system.

Still & Boyd (2004) used a different method to measure individual cycle lengths in the long-term period of Her X-1. To study variability in the long-term period, they calculated an overall long-term ephemeris from many cycles and then used this ephemeris to build an "observed minus computed" diagram for all instances in which the source was seen to be in the "main-on" high flux state. They found that this more local, cycle-to-cycle variability analysis revealed a resetting of the accretion disk clock between anomalous low states in the system, whereas a STWFT analysis had appeared to in-

dicate only a phase shift. This and the previous example justify the use of a local timescale analysis rather than Fourier or even STWFT analysis in order to accurately extract the fine details of time variability in non-periodic systems.

From the ASM light curve of LMC X-3 (Figure 1) it is clear that simply setting a maximum or minimum count rate threshold and counting cycles as occurring between either successive minima or maxima would result in missing some cycles altogether and double-counting others, due to the complex variability. Some maxima are much higher than others, some minima much lower. However, the times when the mean-subtracted signal changes value from negative to positive are quite smooth and well behaved. Because of this, we adopt the method of measuring zero crossings to characterize the cycle-to-cycle variability of LMC X-3. Zero crossing analysis, a specific form of the more general level crossing analysis, is a well accepted local time signal analysis technique used in a wide variety of arenas, from speech processing to oceanography to image analysis (Rabiner & Schafer 2007; Rychlika & Aberga 2007; US Army Corps of Engineers 2008; Zhang, Yang & Yang 2010).

Due to the significant spread in the value of the maxima of the LMC X-3 light curve, and the fact that the minima are poorly defined due to their intrinsically low count rate, the zero crossings are the most easily localizable characteristic points in the signal, and identifying these leads to the most straightforward estimate of the cycle length from one oscillation to the next.

We find the time of each upward and downward zero crossing by calculating the slope of the signal between adjacent points in time where the sign changes from negative to positive or vice versa. The slopes are then used to linearly interpolate to the time at which the signal would have a value of zero. These are the zero crossings. The "period" for each long-term excursion is defined as the time between two successive up-crossings (or two successive down-crossings). The "amplitude" for each long-term excursion is defined as the maximum minus the minimum flux value between two successive crossings. For each cycle, two measurements of the period and amplitude can be made, one using upcrossings and one using downcrossings. Both approaches yield the same results within the errors.

For a simply repeating, symmetric function such as a sine wave, the period derived from the time between successive upcrossings would be identical to that derived from successive downcrossings. Similarly, the amplitude derived from the extrema between upcrossings would be identical to that derived from the extrema between downcrossings. For a time series such as LMC X-3, where the signal is not periodic and the morphology of each flux excursion from one crossing to the next is often far from symmetric, the individual periods derived from individual upcrossings may vary significantly from those derived from neighboring downcrossings (see Figure 4).

In the smoothed ASM lightcurve, LMC X-3 undergoes 14 upcrossings (and so contains 13 upcrossing periods, where a period is defined as the time between two successive upcrossings) and 15 downcrossings (14 downcrossing periods) in the early segment of the light curve. For the middle segment, there are 14 upcrossing periods and 14
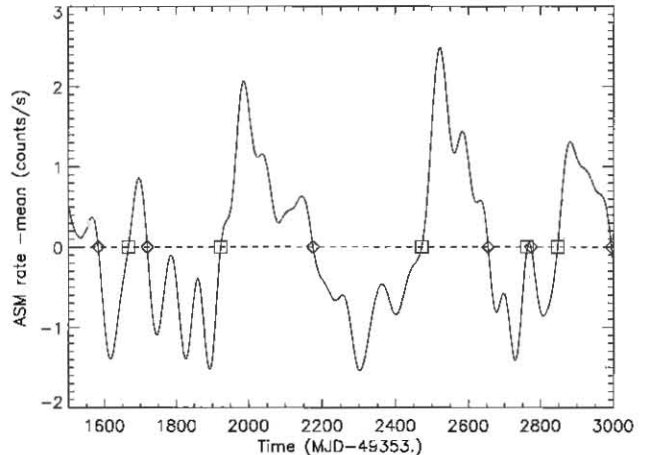

FIG. 4.— A segment of the mean-subtracted, smoothed ASM light curve (solid line) is shown, with calculated times of zero upcrossings (square symbols) and downcrossings (diamond symbols) indicated. For irregular waves, in which the period and amplitude vary from one wave to the next, the time between successive upcrossings or downcrossings can be used to characterize the average period. Note that, while differences are expected between the individual period values obtained from the upcrossing versus downcrossing method, both methods yield statistically similar values for period and amplitude for irregular wave trains.

downcrossing periods. For the late segment, there are three upcrossings (two upcrossing periods) but only two downcrossings (and thus one single downcrossing period).

We use these measured periods to compare the characteristics of the long-term variability, as given by its average amplitude and period, in the early, middle, and late data segments. Figure 5 shows the measured period and amplitude for each long-term flux excursion as defined by upcrossings (squares) and downcrossings (diamonds). Table 1 lists the average period and amplitude derived from both the upcrossing and downcrossing method, for the early, middle and late data segments. While the individual values of period and amplitude vary for the upcrossing versus downcrossing method, their average values are within the errors (Figure 6). The errors are calculated from the standard deviation of the period values from the mean, divided by the square root of the number of cycles, N, in the data segment. During the early data segment before ALS1, the average value of the period is 213±36 days (upcrossing), and 204±35 days (downcrossing). Between ALS1 and ALS2 (i.e., the middle segment), the average period drops by around 80 days and the dispersion from the mean falls three times lower than in the early segment to 119±10 days (upcrossing) and 118±10 days (downcrossing). We note from Figure 5 that the first few periods of the middle data segment are higher than the middle average, and closer to the early average. However there is no excursion in the middle segment that reaches the longer excursion lengths that are commonly seen in the early segment. Our analysis suggests that the early segment and middle segment are statistically different, however there is not enough data to definitively conclude that the change in variability characteristics is directly linked to the ALS's.

After exiting ALS2, there are only 2 upcrossing periods and a single downcrossing period in the smoothed ASM light curve. These are listed in the table for comparison. Although there are too few cycles for statistical signifi-
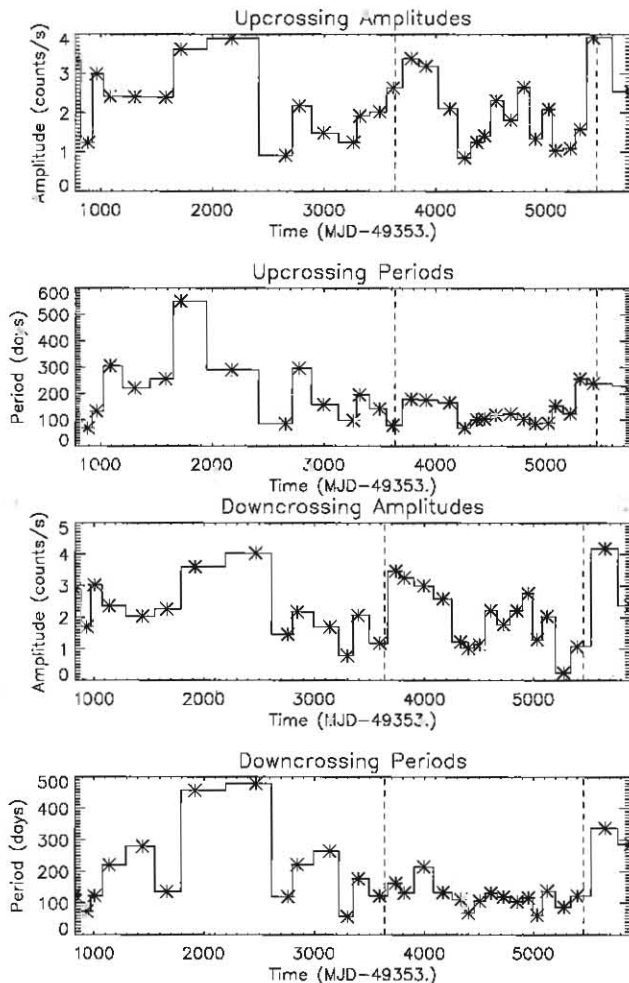
FIG. 5.— Wave-by-wave amplitudes (upper panel) and periods (lower panel) derived from successive upcrossings and downcrossings. The vertical dashed lines represent the mission start dates of ALS1 and ALS2. The amplitudes, and in particular the periods, can be seen to change their behavior after ALS1 (they cluster around a lower mean value, and their dispersion is lower).

cance, the available data suggests that after ALS2, LMC X-3 reenters a state that is more similar to the early segment, with a longer period and higher amplitude, than the middle segment which was characterized by a more tightly bound value of a lower period, as well as a slightly lower amplitude. Note also that the average period and amplitude appear to be monotonically related. This also appears to be the case for individual cycles (Figure 7). As a general rule, excursions with a longer period show a higher amplitude. In particular, there are no occurrences of an individual period longer than about 300 days whose amplitude is lower than 2 counts s^{-1}. Similarly an amplitude below about 1 count s^{-1} has never been seen to occur with a period longer than about 100 days.

3. DISCUSSION

3.1. *Anomalous Low States*

What is the physical state of the accretion disk in LMC X-3 during the anomalous low states? Because the *RXTE* PCA is insensitive to spectral components softer than ~3 keV we cannot use these data to pro-

vide robust constraints on a disk in its low-temperature, low-flux states; a soft excess due to cool-disk emission from an optically thin but geometrically thick accretion disk in the low/hard state would lie beneath this energy cutoff. However, in the low/hard states of GX 339-4, Cyg X-1, and Swift J1753.5−0127, Miller et al. (2006) find evidence for a standard cool accretion disk extending to the innermost stable circular orbit, down to L_x ~0.01L_{Edd}. For values of 0.001L_{Edd} and below, models predict that the entire inner disk may evaporate (Liu et al. 2007; Taam et al. 2008). In addition, iron line studies of GX339-4 at low L_x show that the inner disk edge moves sharply outwards as L_x decreases from 0.01L_{Edd} to 0.001L_{Edd} (Tomsick et al. 2009). For LMC X-3 during ALS1, where the upper limit on the derived total unabsorbed flux is below 0.0005L_{Edd} for an extended period, it seems likely that the inner accretion disk has evaporated and is no longer present.

3.2. *The Long Term Variability*

From Figure 1, it appears that the amplitude of the long-term variability is lower than average in the one or two cycles just prior to each of the two ALS's. A similar trend occurs in Her X-1 just prior to the start of its ALS's. This suggests that the entry into an ALS is not instantaneous, but rather occurs in response to a slow decrease in the accretion rate onto the central source. This then produces a decrease in the flux from the central black hole, which could in principle bring it below the critical value for which irradiation-driven disk warping can occur (Wijers & Pringle 1999; Foulkes, Haswell & Murray 2010).

In Her X-1 Still & Boyd (2004) found that the amplitude of the long-term variability directly scaled with the period of the ~35-day modulation, based on the analysis of three separate anomalous low states observed in BATSE and ASM light curves between 1991 and 2004. Within the uncertainties, this period-amplitude relation appears to also be present in LMC X-3. The behavior between the ALS's appears to follow the same pattern, lending support to the idea that the physical states of the accretion disk before, during and after an ALS are similar in Her X-1 and LMC X-3, even though only Her X-1 is consistent with stable disk precession. For Her X-1, Still & Boyd (2004) interpret this as suggesting that the accretion disk becomes so tightly wound that the effective radiation pressure felt by the disk is reduced. Since the surface area on the disk incident to the compact object decreases with increasing warp, the precession period is then directly correlated with the flux of the compact object.

In general, nonlinear oscillators can be characterized by the relation between the period and amplitude. In the linear regime, the period of a simple oscillator such as a pendulum or spring is independent of the amplitude, however this is not the case in the nonlinear regime. In particular, soft spring oscillators (those that become less resilient with elongation) have a period correlated with the amplitude of the oscillation. For stiff springs, the reverse correlation is present. We conjecture that the same period-amplitude relation is observed in LMC X-3 and Her X-1 because the dynamics of the accretion disks in the two systems are governed by a similar physical process. Furthermore, the existence of a direct

TABLE 1
MEAN PERIODS AND AMPLITUDES FROM ZERO CROSSINGS.

	Period dy	Period Error dy	Amplitude (counts s^{-1})	Amp.Error (counts s^{-1})	N
Early Up	213	36	2.31	0.26	13
Early Down	204	35	2.23	0.24	14
Middle Up.	119	10	1.94	0.22	14
Middle Down	118	10	1.85	0.23	14
Late Up	233	5	3.23	0.69	2
Late Down	287	-	2.36	-	1
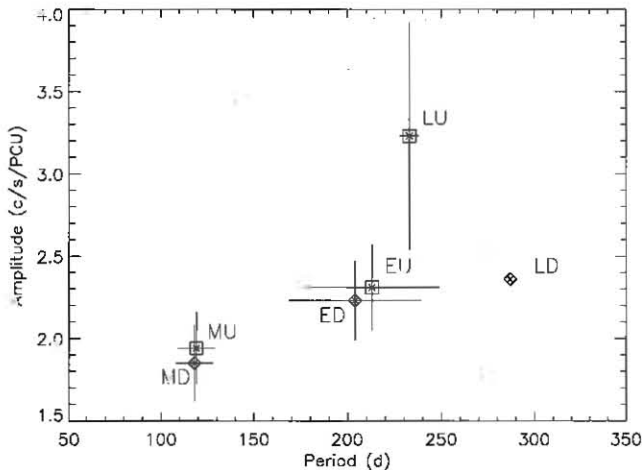
FIG. 6 — The average amplitude versus average period, derived from upcrossings (labeled with U; marked with squares) and downcrossings (D; diamonds) for early (E), middle (M) and late (L) data segments. For the late segment there are only two upcrossing waves and a single downcrossing wave. Since the error bars represent the standard deviations from the mean, the late downcrossing point has no error bar.

FIG. 7.— Wave amplitude versus period for each excursion, as derived from the zero-crossing analysis. Data points marked with diamonds correspond to downcrossings, those with squares to upcrossings. The period and amplitude appear to be monotonically related. Excursions with longer periods have higher amplitudes. There are no occurrences of an individual period longer than about 300 days whose amplitude is lower than 2 counts s^{-1}. Similarly an amplitude below about 1 count s^{-1} has never been seen to occur with a period longer than about 100 days.

correlation between period and amplitude might be predicted by some models of accretion disk dynamics, and not by others. This means that observational results in such systems may give us direct information about the underlying physics. For example, the magnetorotational instability (MRI) is described mathematically in the form of an oscillator, and has been shown to support chaotic solutions (see e.g. Winters, Balbus & Hawley (2003); Umurhan, Regev & Menou (2007)), and under some initial conditions to drive the development of disk dynamos (Kapyla & Korpi 2011). This is closely related to the mechanism that is thought responsible for the disk viscosity, namely, the Balbus-Hawley MHD dynamo (Balbus & Hawley 1991). In this scenario, when a disk possesses ionized hydrogen the MHD dynamo operates, and localized regions of magnetic reconnection at the surface of the disk cause sufficient electron heating to generate the hard X-ray tail. Measuring observationally a well constrained value for the period-amplitude dependence, coupled with spectral diagnostics (such as a hard tail) may thus allow us to place some meaningful physical limits on the presumed mechanisms responsible for both driving and damping the disk oscillations, such as the electric charge density of the disk material, and the strength of the disk magnetic field.

Not only do the average amplitudes in LMC X-3 increase with increasing period, but we have shown this relation seems to hold for individual excursions as well (Figure 7). This could point to the possibility that the
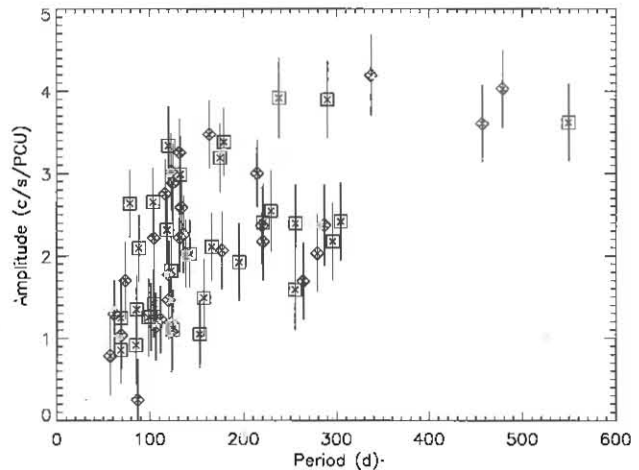
disk is more similar to a so-called "chaotic sea" (used to characterize ocean dynamics) than to a solid precessor, but hundreds of long-term cycles would need to be observed before the distribution of cycle heights and periods could be fit and compared to the expectations. A similar cycle-to-cycle variability was noted in the distribution of long-term variability excursions in the neutron star X-ray binary SMC X-1 by Trowbridge, Nowak & Wilms (2007).

Foulkes, Haswell & Murray (2010) present the results of 3D SPH simulations, using realistic parameters for a wide range of X-ray sources. They find that a generic flat disk is unstable to development of a warping mode, and show that warped, precessing accretion disks occur more commonly in X-ray binary systems than previously thought. In addition, their simulations show that SMC X-1, Cyg X-2 and LMC X-3 - three systems that all show varying long-term cycle lengths - all develop disks with a similar maximum disk warp angle, disk tilt angle, and location of maximum warp position. These three systems are all modeled by Foulkes, Haswell & Murray (2010) as having very high compact object fluxes. To describe the variable long-term cycle length in SMC X-1, Trowbridge et al considered the possibility that the average radius at which accreted material is injected into the disk could vary from one long-term cycle to the next, as suggested by Ogilvie & Dubus (2001). In fact, the simulations of

Foulkes, Haswell & Murray (2010) support this suggestion by revealing that, once precessing, the disk will continuously flex in response to changes in the orientation of the Roche potential, which results in changing the location of the accretion injection stream on the disk.

4. CONCLUSIONS

The 15-year *RXTE* ASM monitoring data show that LMC X-3 has entered into two distinct, extended low/hard states that share several characteristics with the anomalous low states seen in Her X-1. The characteristic amplitude and period of the long-term variability seen in LMC X-3 is measurably different between ALS's. These differences can be characterized statistically by calculating average excursion lengths and amplitudes from a zero-crossing analysis applied to the three segments of data. We find that the characteristic timescale is monotonically related to the characteristic amplitude. A similar relation is also present in Her X-1, and this relation is in the same direction in each system. We interpret this as suggestive that the accretion disk dynamics of LMC X-3 is on some level analogous to that in Her X-1, even though the two sources contain a different type of compact object at their centers. Whatever physical process is driving the dynamics of the accretion disk resulting in the observed long-term variability observed in Her X-1 may also be the dominant process responsible for the long-term variability seen in LMC X-3. Analysis of the variability in both systems suggests that this mechanism must be sensitive to the initial conditions when the geometry governing the dynamics is re-established, such as after ALS's. The existence of a unifying mechanism giving rise to the long-term variability in two very different systems - pulsar versus black hole - may help to elucidate the process governing this still poorly understood characteristic of many X-ray binaries, and tie it to a family of nonlinear oscillators of a certain form.

Wilms et al. (2001) found that the specific long-term flux and spectral variations of LMC X-3 could be well modelled by an accretion disk wind-driven limit cycle driven by Compton heating, as proposed by Shields et al.

(1986). In this scenario, under certain circumstances that depend on the masses of the system parameters, the accretion rate can become so high that as a result the compact object develops a wind sufficiently strong to temporarily halt accretion. This loss of fuel propagates forward in time, lowering the X-ray flux and damping the wind, which then allows the accretion rate to again increase, the recurrence happening on the viscous timescale. Since this model includes a both damping and driving mechanisms, it deserves further investigation to see if it could give rise to the behavior seen in LMC X-3 and Her X-1.

Cycle-to-cycle variability is a hallmark of the long-term flux evolution in a number of X-ray binary systems. However, characterizing this variability is only possible with the existence of nearly continuous, nearly evenly sampled lightcurve data on timescales longer than the characteristic period of the variability under study. The *RXTE* ASM has been the workhorse instrument in providing such data, and we are now at the point where nonlinear time series analysis techniques can be applied to real astrophysical data with variability timescales of hundreds of days. With the quality of data in hand it should soon be possible to extend this analysis to many other systems that show high amplitude non-periodic long-term variability, to search for other examples of such a period-amplitude relation, which could point to an underlying physical mechanism that unlocks the secrets of accretion disk dynamics.

REFERENCES

Abell, G.O. & Margon, B., 1979, Nature, 279, 701

Balbus, S.A. & Hawley, J.E. 1991, ApJ, 376, 214

Balbus, S.A. & Hawley, J.E., 2003, LNP, 614, 329

Boyd, P.T., Smale, A.P., Homan, J., Jonker, P.G., & van der Klis, M. 2000, ApJ, 542, L127

Boyd, P. T. & Smale, A. P., 2004, ApJ, 612, 1006

Bradt, H.V., Rothschild, R.E. & Swank, J.H., 1993, A&AS 97, 355

Brocksopp, C., Groot, P.J. & Wilms, J., 2001, MNRAS, 328, 1398

Chen, X., & Taam, R.E. 1996, ApJ, 466, 404

Clarkson, W.I., Charles, P.A., Coe, M.J., Laycock, S., Tout, M.D., & Wilson, C.A., 2003, MNRAS, 339, 447

Cowley, A.P., Crampton, D., Hutchings, J.B., Remillard, R., & Penfold, J.E., 1983, ApJ, 272, 118

Cowley, A.P., Schmidtke, P.C., Ebisawa, K., Makino, F., Remillard, R.A., Crampton, D., Hutchings, J.B., Kitamoto, S. & Treves, A., 1991, ApJ, 381, 526

Cowley, A.P., Schmidtke, P.C., Hutchings, J.B. & Crampton, D., 1994, ApJ, 429, 826

Cui, W., Feng, Y.X., Zhang, S.N., Bautz, M.W., Garmire, G.P., & Schulz, N.S., 2002, ApJ, 576, 357

Durant, M., Cornelisse, R., Remillard, R. & Levine A., 2010, MNRAS, 401, 355

Fabian, A.C. & Rees, M.J., 1979, MNRAS, 187, 13P

Foulkes, S.B., Haswell, C.A. & Murray, J.R., 2010, MNRAS, 401, 1275

Gilmore, R. 1998, Rev.Mod.Phy, 70, 1455

Gotz, D., Mereghetti, S., Merlini, D., Sidoli, L., & Belloni, T., 2006, A&A, 448, 873

Gruber, D.E. & Rothschild, R.E., 1984, ApJ, 283, 546

Jahoda, K., Swank, J.H., Giles, A.B., Stark, M.J., Strohmayer, T., Zhang, W. & Morgan, E.H., 1996, in EUV, X-ray and Gamma-Ray Instrumentation for Astronomy VII, ed. O.H. Siegmund (Bellingham: SPIE), 59

Kapyla, P.J. & Korpi, M.J., 2011, MNRAS, 413, 901

Lang, F.L., Levine, A.M., Bautz, M., Hauskins, S., Howe, S., Primini, F.A., Lewin, W.H.G., Baity, W.A., Knight, F.K., Rothschild, R.E. & Petterson, J.A., 1981, ApJ, 246, L21

Levine, A. M., Bradt, H., Cui, W., Jernigan, J.G., Morgan, E.H., Remillard, R., Shirey, R.E. & Smith, D.A., 1996, ApJ, 469, L33

Liu, B. F., Taam, R. E., Meyer-Hofmeister, E., & Meyer, F., 2007, ApJ, 671, 695

Miller, J. M., Homan, J., Steeghs, D., Rupen, M., Hunstead, R. W., Wijnands, R., Charles, P. A., & Fabian, A. C., 2006, ApJ, 653, 525

Nowak, M. A., Wilms, J., Heindl, W. A., Pottschmidt, K., Dove, J. B., & Begelman, M. C., 2001, MNRAS, 320, 316

Ogilvie, G.I. & Dubus, G., 2001, MNRAS, 320, 485

Page, M. J., Soria, R., Wu, K., Mason, K. O., Cordova, F. A., & Priedhorsky, W. C., 2003, MNRAS, 345, 639

Paul, B., Kitamoto, S. & Makino, F., 2000, ApJ, 528, 410

Points, S.D., Chu, Y.-H., Snowden, S.L., & Smith, R.C., 2001, ApJS, 136, 99

Priedhorsky, W.C. & Holt, S.S., 1987, Space Sci.Rev., 45, 291

Rabiner, L.R. & Schafer, R.W., 2007, "Introduction to Digital Speech Processing", Foundations and Trends in Signal Processing: Vol. 1: No 12, 1-194

Rots, A.H., Jahoda, K. & Lyne, A.G., 2004, ApJ, 605, L129

Rychlika, I. & Aberga, S., 2007, Note on the intensity of encountered waves, Ocean Engineering, Volume 34, Issues 11-12, August 2007, 1561-1568

Shields, G.A., McKee, C.F., Lin, D.N.C. & Begelman, M.C., 1986, ApJ, 306, 90

Smith, D. M., Dawson, D. M., & Swank, J. H., 2007, ApJ, 669, 1138

Soria, R., Wu, K., Page, M.J. & Sakelliou, 2001, A&A, 365, L273

Steiner, J.F., McClintock, J.E., Remillard, R.A., Gou, L., Yamada, S., & Narayan, R., 2010, ApJ, 718, L117

Still, M. & Boyd, P. 2004, ApJ, 606, L135

Taam, R. E., Liu, B. F., Meyer, F., & Meyer-Hofmeister, E., 2008, ApJ, 688, 527

Tomsick, J.A., Yamaoka, K., Corbel, S., Kaaret, P., Kalemci, E. & Migliari, S., 2009, ApJ, 707, L87

Trowbridge, S., Nowak, M.A. & Wilms, J., 2007, ApJ, 670, 624

Umurhan, O.M., Regev, O. & Menou, K., 2007, Phys.Rev.E, 76, 036310

US Army Corps of Engineers, Costal Engineering Manual, 2008, Part II, Chapter 1

Val-Baker, A.K.F., Norton, A.J. & Negueruela, I, 2007, AIPC, 924, 530

Wijers, R.A.M.J. & Pringle, J.E., 1999, MNRAS, 308, 207

Wilms, J., Nowak, M.A., Pottschmidt, K., Heindl, W.A., Dove, J.B. & Begelman, M.C., 2001, MNRAS, 320, 327

Winters, W.F., Balbus, S.A., & Hawley, J.F., 2003, MNRAS, 340, 519

Wojdowski, P.S., Clark, G.W. & Kallman, T.R., 2000, ApJ, 541, 963

Wu, K., Soria, R., Page, M.J., Sakelliou, I., Kahn, S.M., & de Vries, C.P., 2001, A&A, 365, L267

Zhang, M., Li, X., Yang, Z. & Yang, Y., 2010, A novel zero-crossing edge detection method based on multi-scale space theory in Signal Processing (ICSP), 2010 IEEE 10th International Conference on, 1036-1039